Dentistry 3000

Vol 13 No 1 (2025) DOI 10.5195/d3000.2025.866

The Impact of Thermocycling on the Physio-mechanical Properties of SLA and DLP 3D-Printed Dental Ceramics: A Comparative Study

Nadia H Hasan

College of Dentistry, University of Mosul, Mosul, Iraq

Abstract

Objective: Three-dimensional (3D) printing technology is highly promising for producing nanoceramic resin dental restorations. However, the effects of environmental stressors on the structural integrity and clinical performance of these restorations require further elucidation. To investigate the effects of Stereolithography (SLA) and digital light processing (DLP) 3D printing technologies on the physical-mechanical properties of a 3D-printed resin material used in dental applications.

Methods: A total of 120 resin specimens (Senertek P-Crown V2) were fabricated using SLA and DLP technologies. The microhardness, flexural strength, and surface roughness of the specimens were evaluated under control and thermocycling conditions to evaluate their long-term performance. To assess statistical significance a two independent sample t-tests ($P < 0.05$) were used to analysis the data.

Results: SLA samples exhibited significantly higher microhardness ($P = 0.001$) and flexural strength than DLP samples, both in the control state and after thermocycling. After thermocycling, the microhardness of SLA samples increased, whereas that of DLP samples decreased. Surface roughness values increased significantly in both SLA and DLP samples after thermocycling, with SLA samples exhibiting higher roughness values.

Conclusion: SLA-printed resin demonstrated superior microhardness and flexural strength compared to DLP-printed resin. However, its long-term durability is affected by immersion and thermocycling. This study highlights the impact of water sorption, polymerization mechanisms, and surface morphology on material performance.

Keywords: 3D printing, dental materials, digital light processing, flexural strength, microhardness, stereolithography, surface roughness, thermocycling.

Citation: Hasan NH. (2025) The Impact of Thermocycling on the Physio- mechanical Properties of SLA and DLP 3D-Printed Dental Ceramics: A Comparative Study. Dentistry 3000. 1:a001 doi:10.5195/d3000.2025.866
Received: February 27, 2025
Accepted: March 31, 2025
Published: April 21, 2025

Email: nadiahameed@uomosul.edu.iq.

Introduction

Stereolithography (SLA) and digital light processing (DLP) are 3D printing dental techniques requiring high resolution and accuracy. Despite their similarities in using volume-accelerated technology (VAT) to create accurate dental restorations, but differ in speed, resolution, and cost-effectiveness [1].

Ultraviolet light uses to solidify a resin in both SLA and DLP but different method [2,3]. A resistance to daily exposure to an intense condition of the oral environment, is a significant factor for the successful clinical use of a nano ceramic materials that impact it's the morphological, physical, mechanical properties cause surface integrity degradation [4,5].

A higher microhardness enhances wear resistance, while excessive surface roughness can weaken flexural strength by creating stress concentration points [6,7], and an optimal balance through material selection and technique- processing is essential to improving ceramic durability, structural reliability [8].

The study aimed to compare the SLA and DLP methods with regards to their physical-mechanical properties and the influence of artificial aging. The

Dentistry 3000
Vol 13 No 1 (2025) DOI 10.5195/d3000.2025.866

null hypothesis stated that both 3D printing techniques showed no difference in such properties.

Material and Methods

The samples used in this study were divided as depicted in Figure 1.

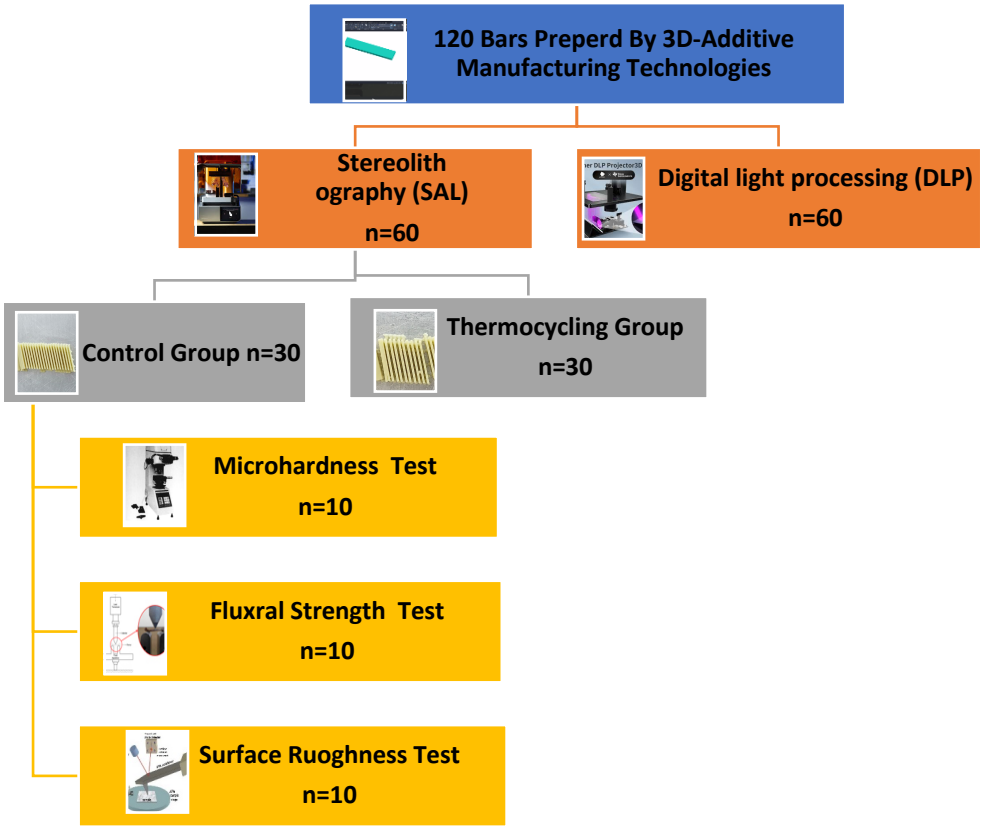

Figure 1. Schematic diagram of the study design.

Ethical considerations

All study participants provided informed consent, and the study design was performed solely on laboratory models; therefore, informed consent was not required confidentiality, and procedures for withdrawal from the research.

Measures

A total of 120 rectangular bars (25 × 5 × 1 mm) were prepared using the Senertek P-Crown V2 resin material (Libral Traders, India). To design the bar geometry, AutoCAD software was used and saved as a standard tessellation language (STL) file. The STL file was utilized in the Anycubic Photon Mono 2 and Anycubic Photon D2 3D printers (Lux Creo Inc., Chicago, IL, USA), which use SLA and DLP technologies, respectively, to produce 60 bars from each technique (Figure 1).

The STL file was processed using a slicer program that converted it into G-code for machine readability [9]. The samples were constructed with resolutions as fine as 50 microns, ensuring precise detailing.

Dentistry 3000
Vol 13 No 1 (2025) DOI 10.5195/d3000.2025.866

After printing, the samples were cured in an ultraviolet oven for 8 minutes in a clear jar filled with glycerin, to improve the mechanical properties and ensure complete solidification. Post-processing steps included sanding, painting, polishing, tumbling, high-pressure air cleaning, and coloring to make the 3D model ready for application [10].

In SLA, a perforable platform was positioned adjacent to the VAT containing liquid polymer resin. A laser beam was directed onto the platform, solidifying the first layer of resin.

The platform was then incrementally lowered to form subsequent layers, repeating until the 3D object was fully constructed, taking approximately 38 minutes. SLA requires support structures to stabilize the model during printing. DLP is like SLA, with the primary distinction being the light source. DLP employs a conventional light source and digital micromirrors to print all the layers simultaneously. This approach allows faster printing compared to SLA, where the laser traces the cross-sectional area point by point. [11,12].

Sixty rectangular bars (30 from each technique) underwent thermocycling in a thermocycling unit (Dorsa apparatus, Tehran, Iran) from 5 °C to 55 °C for 1,000 cycles with a 30 second dwell time, to simulate approximately 1 year of intraoral use [13]. The microhardness, flexural strength, and surface roughness of the nanoceramic resin material were evaluated in 40 rectangular bars per test (20 bars from each 3D printing technique: 10 as control group and 10 after thermocycling).

The microhardness of the nanoceramic resin bars was evaluated by subjecting the centre of each bar to three indentations using a diamond pyramid indenter. A load of 300 g was applied for 10 s to determine the Vickers Hardness Number in kg/mm² [13]. The mean values of these measurements were calculated using a DM 8/DM 2 microhardness tester (Yang Yi Technology Co., Ltd, Tainan City 70960, Taiwan) (Figure 2).

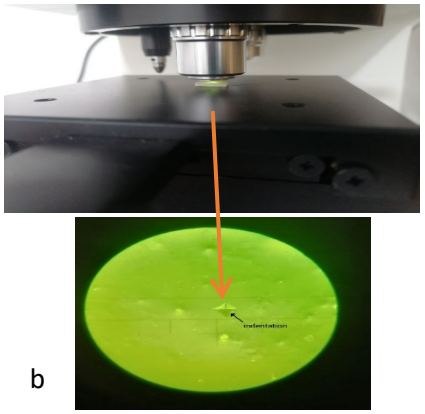

Figure 2: (a) Vickers micro-indentation testing machine, (b) image of indentation.

Using a universal testing machine, flexural strength of the nanoceramic resin bars was assessed. On two supporting bearers each bar was placed with its intaglio surface facing downward, following ISO standards [14].

A 1.6 mm spherical-tipped indenter applied force centrally on a 5-mm wide face, perpendicular to the bar's longitudinal axis. The load required to fracture each bar was recorded to the nearest 0.1 N, with a force application rate not exceeding 0.5 N/s (Figure 3).

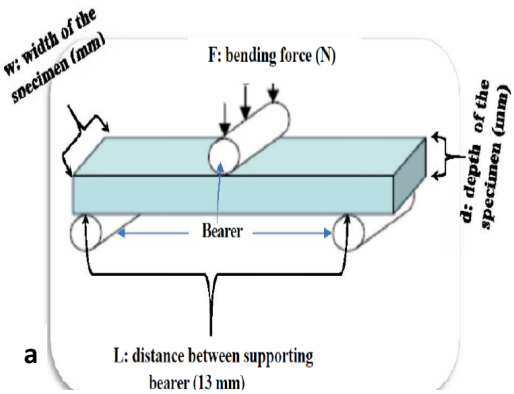

Figure 3: (a) schematic diagram of the three-point flexural strength test apparatus, (b) image of universal testing machine and testing bar.

Dentistry 3000
Vol 13 No 1 (2025) DOI 10.5195/d3000.2025.866

Tests were conducted in a dry environment, and flexural strength was calculated using the standard equation [14,15].

$$\sigma = 3\,FL/2\,wd2\ N/mm^2 \text{ or } MPa$$

Where σ (sigma) represents stress in MPa; F, the applied force (N); L, length or distance over which the force is applied (mm); w, width of the element affected by the stress (mm); and d, depth or thickness of the element (mm).

Using the touch approach of an atomic force microscope (FlexAFM, Nanosurf AG, Liestal, Switzerland) , an intaglio surfaces of the nanoceramic resin bars were analysed for surface topography. The three central readings per bar were recorded, and surface roughness value (Sa) was calculated. A 3D image covering an area of 20,000 × 20,000 nm was captured (Figure 4).

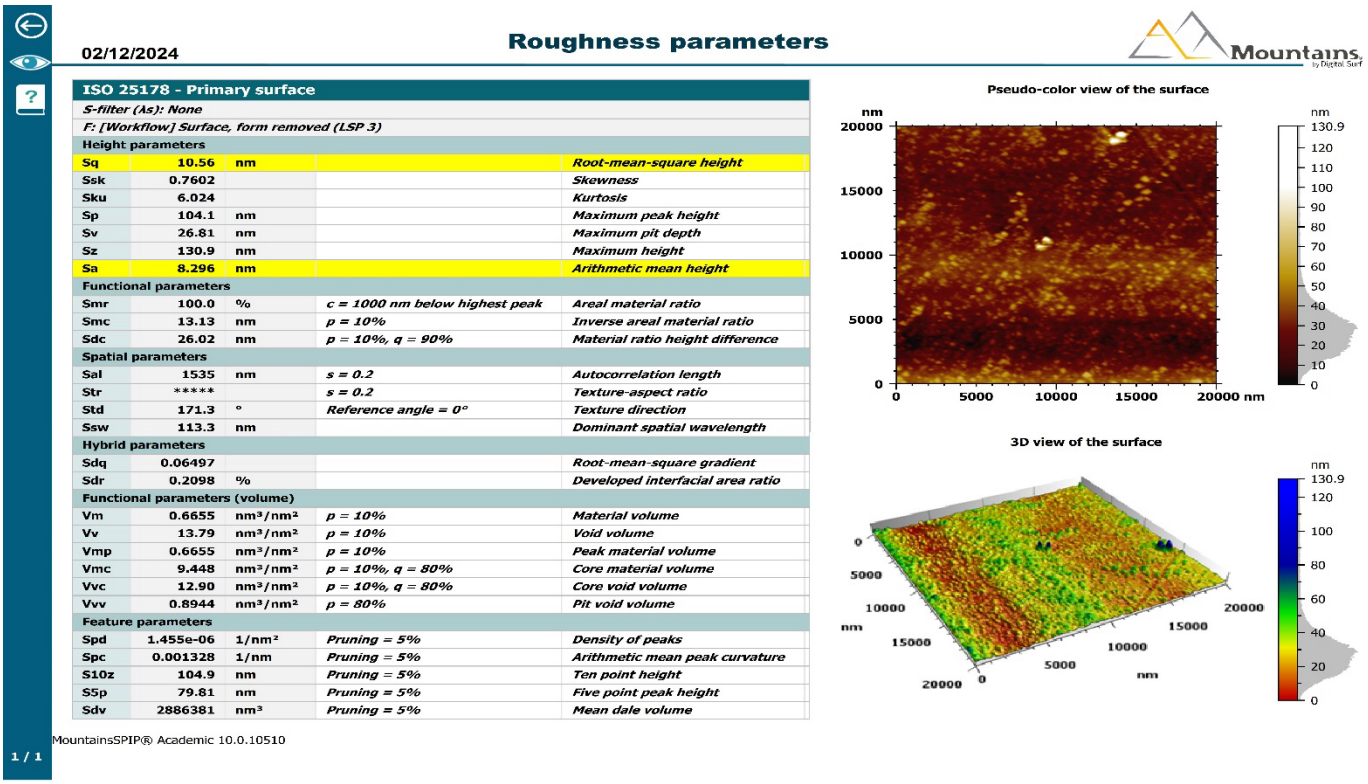

02/12/2024

Roughness parameters

Mountains

ISO 25178 - Primary surface				
S-filter (As): None				
F: [Workflow] Surface, form removed (LSP 3)				
Height parameters				
Sq	10.56	nm		*Root-mean-square height*
Ssk	0.7602			*Skewness*
Sku	6.024			*Kurtosis*
Sp	104.1	nm		*Maximum peak height*
Sv	26.81	nm		*Maximum pit depth*
Sz	130.9	nm		*Maximum height*
Sa	8.296	nm		*Arithmetic mean height*
Functional parameters				
Smr	100.0	%	*c = 1000 nm below highest peak*	*Areal material ratio*
Smc	13.13	nm	*p = 10%*	*Inverse areal material ratio*
Sdc	26.02	nm	*p = 10%, q = 90%*	*Material ratio height difference*
Spatial parameters				
Sal	1535	nm	*s = 0.2*	*Autocorrelation length*
Str	*****		*s = 0.2*	*Texture-aspect ratio*
Std	171.3	°	*Reference angle = 0°*	*Texture direction*
Ssw	113.3	nm		*Dominant spatial wavelength*
Hybrid parameters				
Sdq	0.06497			*Root-mean-square gradient*
Sdr	0.2098	%		*Developed interfacial area ratio*
Functional parameters (volume)				
Vm	0.6655	nm³/nm²	*p = 10%*	*Material volume*
Vv	13.79	nm³/nm²	*p = 10%*	*Void volume*
Vmp	0.6655	nm³/nm²	*p = 10%*	*Peak material volume*
Vmc	9.448	nm³/nm²	*p = 10%, q = 80%*	*Core material volume*
Vvc	12.90	nm³/nm²	*p = 10%, q = 80%*	*Core void volume*
Vvv	0.8944	nm³/nm²	*p = 80%*	*Pit void volume*
Feature parameters				
Spd	1.455e-06	1/nm²	*Pruning = 5%*	*Density of peaks*
Spc	0.001328	1/nm	*Pruning = 5%*	*Arithmetic mean peak curvature*
S10z	104.9	nm	*Pruning = 5%*	*Ten point height*
S5p	79.81	nm	*Pruning = 5%*	*Five point peak height*
Sdv	2886381	nm³	*Pruning = 5%*	*Mean dale volume*

MountainsSPIP® Academic 10.0.10510

1 / 1

Figure 4. Roughness parameters.

Statistical analysis

For statistical analysis of data distribution, the microhardness, flexural strength, and surface roughness values were statistically analyzed using SPSS Statistics 27.0 (IBM Corp., Armonk, NY, USA). Parametric independent sample t-tests were used to compare the effect of each variable and determine statistical differences between groups, with 95% confidence level and $P \leq 0.05$ considered statistically significant.

Results

Participant characteristics

To determine the sample size a software (G*Power) used, at $\alpha = 0.05$ and $1-\beta = 0.80$, with an expected effect size of 0.3.

Descriptive statistics

The impact of thermocycling on the physical-mechanical

Dentistry 3000
Vol 13 No 1 (2025) DOI 10.5195/d3000.2025.866

properties of 3D-printed Senertek P-Crown V2 resin material was determined. Tables 1 and 2 present the descriptive statistics, including mean, standard deviation, and campers' mean, of the microhardness, flexural strength, and surface roughness of 3D-printed resin samples to assess the impact of control and thermocycling states on SLA and DLP technologies and vice versa, respectively. Two independents sample t-tests ($P < 0.05$) were conducted to assess the significance of the results.

Correlation among variables

As shown in Table 1, after thermocycling, the microhardness values were higher in SLA samples (0.71153 kg/mm²) compared to DLP samples, whereas DLP samples had significantly higher values in the control state (0.32602 kg/mm²). Higher mean flexural strength values (24.5080 MPa, 5.3940 MPa) were obtained for SLA samples compared to DLP samples, respectively, in both the control state and after thermocycling.

Finally, the highest mean value for surface roughness (Sa value) was obtained for SLA samples that underwent thermocycling.

Table 1. Descriptive statistics and camper mean of flexural strength, microhardness, and surface roughness values for both stereolithography and digital light processing 3D printing technologies.

TEST			N	Mean	Std. Deviation	Std. Error Mean	T-test	P value
Flexural Strength value	DLP	Control	10	19.7040	0.95789	0.30291	0.298	0.772
		Thermocycling	10	20.1170	4.27474	1.35179		
	SLA	Control	10	24.5080	1.04583	0.33072	1.258	0.225
		Thermocycling	10	25.3940	1.96681	0.62196		
Microhardness value	DLP	Control	10	18.6250	1.03098	0.32602	3.463	0.004**
		Thermocycling	10	16.3200	1.83473	0.58019		
	SLA	Control	10	16.9720	0.73976	0.23393	2.351	0.039*
		Thermocycling	10	18.7330	2.25007	0.71153		
Surface Roughness Value	DLP	Control	10	4.8087	0.66203	0.20935	3.974	0.002**
		Thermocycling	10	7.1051	1.71642	0.54278		
	SLA	Control	10	5.3585	0.70850	0.22405	9.148	0.000**
		Thermocycling	10	22.5296	5.89325	1.86361		

DLP, digital light processing; SLA, stereolithography

Dentistry 3000
Vol 13 No 1 (2025) DOI 10.5195/d3000.2025.866

Additionally, in shown in Table 2, among DLP samples, higher microhardness values were observed in the control state (18.6250 kg/mm²), whereas the SLA group showed higher values after thermocycling (18.7330 kg/mm²). No significant differences in flexural strength were observed between the control and thermocycling groups for both SLA and DLP technologies. Finally, the increase in Sa values was more pronounced after thermocycling than in the control state for both DLP and SLA technologies (5.3585 µm and 22.5296 µm, respectively).

Table 2. Descriptive statistics and camper mean of flexural strength, microhardness, and Sa surface roughness values for each 3D printing technologies in control and thermocycling states.

TEST			N	Mean	Std. Deviation	Std. Error Mean	T-test	P value
Flexural strength value	Control	DLP	10	19.7040	0.95789	0.30291	10.712	0.000**
		SLA	10	24.5080	1.04583	0.33072		
	Thermocycling	DLP	10	20.1170	4.27474	1.35179	3.546	0.002**
		SLA	10	25.3940	1.96681	0.62196		
Microhardness value	Control	DLP	10	18.6250	1.03098	0.32602	4.119	0.001*
		SLA	10	16.9720	0.73976	0.23393		
	Thermocycling	DLP	10	16.3200	1.83473	0.58019	2.628	0.017*
		SLA	10	18.7330	2.25007	0.71153		
Surface roughness value	Control	DLP	10	4.8089	0.66178	0.20927	1.793	0.09
		SLA	10	5.3585	0.70850	0.22405		
	Thermocycling	DLP	10	7.1051	1.71642	0.54278	7.947	0.000**
		SLA	10	22.5296	5.89325	1.86361		

DLP, digital light processing; SLA, stereolithography

Discussion

In this in vitro comparative study, we investigated the effects of SLA and DLP 3D printing on the physical-mechanical properties of a 3D-printed resin material used in dental applications.

In clinical dentistry, SLA and DLP have become pivotal for fabricating indirect restorations, offering efficiency and material conservation. Both processes enable the production of intricate designs with minimal material waste compared to traditional subtractive manufacturing techniques, yet each exhibits distinct advantages and

limitations depending on the application [16,17]. For instance, challenges such as weak interlayer adhesion and anisotropic material behavior underscore the importance of understanding the nuances of each technology. Choosing between SLA and DLP requires not only technical expertise but also the guidance of knowledgeable partners to optimize production outcomes and achieve high-quality results [18].

During daily use within oral environment, restorations are subjected to thermal stresses and evaluating the effects of 3D-printed resins in simulated oral conditions are important studies to assess the clinical performance of these newly introduced technologies. Bardia et al. [12], reported that when a resin restoration subjecting a to 1,000 cycles of a thermal variation to simulates 1 year of clinical dental use. A plasticizer effect of water sorption of resin affects its mechanical properties. Moreover, increased temperature accelerates water sorption, thereby interfering with its mechanical properties [19].

Salivary pH usually ranges from 6.8 to 7.2; however, dietary acids can cause a drop in salivary pH . A dietary acids hydroxyl ion may diffuse through saliva water molecules, react with resin ceramic oxygen and caused ceramic degradation [5]. Surface hardness is an indicator of a material's abrasion resistance and surface strength. Restorations with low surface hardness are more prone to scratches, damage to the resin surface, and dimensional changes during mechanical dental brushing or chewing hard foods [20]. In our study, DLP samples exhibited low hardness values after thermocycling, probably due to water sorption and alterations in the composition of the material and printing layers under thermal stress. In contrast, the SLA group exhibited a significant increase in hardness with aging compared to the bulkier DLP group, which may be attributed to its layering technique and enhanced polymerization rate, depth of polymerization, and degree of conversion.

The higher flexural strength of the SLA group compared to that of the DLP group indicates its greater resistance to surface deformation and higher flexibility, which may be explained by the differences in the curing mechanisms of DLP and SLA, coupled with differences in surface morphologies [21]. Additionally, a non-significant positive effect in flexural strength after artificial aging was observed for both the DLP and SLA groups, possibly owing to reduced water sorption, which alters a material's characteristics by creating internal tensions that are damaging to a resin's long-term usefulness [22]. Reducing water sorption can prevent breaches and cracks and enhance the longevity of dental restorations. Moreover, remnant monomers in the resin have been linked to dimensional fragility of restorations and may adversely affect oral tissues [23].

Surface roughness is one of the most important properties affecting the longevity of dental restorations. Rougher surfaces increase microbial adhesion, leading to dental stomatitis, and promote surface staining and discoloration, which can compromise dental aesthetics [18]. The surface topography of additively manufacturing materials requires further investigation, as the layering technology impacts the

porosity and morphological features of printed objects [24]. Significant difference in surface roughness existed between the control and thermocycling groups for both the DLP and SLA technologies. According to Al-Dulaijan et al., this difference may be attributable to the deterioration that occurs in the organic matrix or at the matrix-filler interface of dental resins during thermocycling and to the layering technology, which involves multiple steps between adjacent layers[25].

Therefore, the null hypothesis, which posited no differences in microhardness, flexural strength, and surface roughness between SLA- and DLP-printed nanoceramic resin bars even after artificial aging, was rejected.

Conclusion

To conclude, SLA printed resins are preferable for strength, but their roughness value increases with time and their long-term performance needs further study focusing on reducing water sorption and improving resin stability.

Conflicts of interest

The author declares no competing interest.

References

1. Mechanical and biocompatibility properties of 3D-printed dental resin reinforced with glass silica and zirconia nanoparticles: In vitro study. Alshamrani A, Alhotan A, Kelly E, Ellakwa A Polymers 2023; 15:2523.
2. An overview of modern metal additive manufacturing technology. Armstrong M, Mehrabi H, Naveed N. J Manuf Process 2022; 84:1001-1029.
3. Additive manufacturing by digital light processing: a review. Chaudhary R, Fabbri P, Leoni E, Mazzanti F, Akbari R, Antonini C. Prog Addit Manuf 2023; 8:331-351.
4. Lithium disilicate and zirconia reinforced lithium silicate glass-ceramics for CAD/CAM dental restorations: biocompatibility, mechanical and microstructural properties after crystallization. Mavriqi L, Valente F, Murmura G, Sinjari B, Macrì M, Trubiani O, et al. J Dent 2022; 119:104054.
5. Investigation of the influence of gastric acid on the surface roughness of ceramic materials of metal-ceramic restorations. An in vitro study. Matsou E, Vouroutzis N, Kontonasaki E, Paraskevopoulos KM, Koidis P. Int J Prosthodont 2011; 24:26-9.
6. Gastric acid challenge of lithium disilicate–reinforced glass–ceramics and zirconia-reinforced lithium silicate glass–ceramic after polishing and glazing—impact on surface properties. Hjerppe J, Shahramian K, Rosqvist E, Lassila LVJ, Peltonen J, Närhi TO. Clin Oral Investig 2023; 27:6865–6877.
7. Effect of simulated gastric acid exposure on the hardness, topographic, and colorimetric properties of machinable and pressable zirconia-reinforced lithium silicate glass-ceramics. Alhotan A, Alaqeely R, Al-Johani H, Alrobaish S, Albaiz S. J Prosthet Dent 2024; 132:625.e1-625.e7.
8. Flexural strength, fatigue behavior, and microhardness of three-dimensional (3D)-printed resin material for indirect restorations: A systematic review. Abad-Coronel C, Durán Urdiales D, Benalcázar Arias MV, Córdova AK, Medina MS, et al. Materials 2025; 18:556.
9. Additive manufacturing: A comprehensive review. Zhou L, Miller J, Vezza J, Mayster M, Raffay M, Justice Q, et al. Sensors 2024; 24: 2668.

Dentistry 3000
Vol 13 No 1 (2025) DOI 10.5195/d3000.2025.866

10. Evaluating oxygen shielding effect using glycerin or vacuum with varying temperature on 3D printed photopolymer in post-polymerization. Lim JH, Lee SY, Gu H, Jin G, Kim JE. J Mech Behave Biomed Mater 2022; 130:105170.
11. 3D printing in dentistry. Jambhule S, Palandurkar M, Shewale A. Int J Adv Res 2022; 10:742-750.
12. The effect of build angle and artificial aging on the accuracy of SLA- and DLP-printed occlusal devices. Saadat SB, Schmidt F, Beuer F, Metin DS, Simeon P, Nicic R, et al. Polymers 2024; 16:1714.
13. Effect of 3D printing system and post-curing atmosphere on micro- and nano-wear of additive-manufactured occlusal splint materials. Wada J, Wada K, Garoushi S, Shinya A, Wakabayashi N, Iwamoto T, et al. J Mech Behav Biomed Mater 2023; 142:105799.
14. ISO/ASTM 52900: Additive manufacturing — General principles — Fundamentals and vocabulary. 2nd ed. International Organization for Standardization, 2021.
15. Hibbeler RC. Mechanics of materials. 8th ed. Pearson Prentice Hall, Boston, USA; 2010.
16. Additive manufacturing technologies used for processing polymers: Current status and potential application in prosthetic dentistry. Revilla-León M, Özcan M. J. Prosthodont 2019; 28:146-158.
17. Material anisotropy in additively manufactured polymers and polymer composites: A review. Zohdi N, Yang R. Polymers 2021; 13:3368.
18. Fracture load of 3D-printed fixed dental prostheses compared with milled and conventionally fabricated ones: The impact of resin material, build direction, post-curing, and artificial aging: An in vitro study. Reymus M, Fabritius R, Keßler A, Hickel R, Edelhoff D, Stawarczyk B. Clin Oral Investig 2020; 24:701-710.
19. Strength and surface properties of a 3D-printed denture base polymer. Gad MM, Fouda SM, Abualsaud R, Alshahrani FA, Al-Thobity AM, Khan SQ, et al. J Prosthodont 2022; 31:412-418.
20. Effect of post-curing light exposure time on the physico–mechanical properties and cytotoxicity of 3D-printed denture base material. Aati S, Akram Z, Shrestha B, Patel J, Shih B, Shearston K, et al. Dent Mater 2021; 38:57-67.
21. Evaluating and comparing flexure strength of dental models printed using fused deposition modelling, digital light processing, and stereolithography apparatus printers. Atwal N, Bhatnagar D. Cureus 2024; 16:54312.
22. Factors affecting flexural strength of 3D-printed resins: a systematic review. Gad MM, Fouda SM. J. Prosthodont 2023; 32 Supp 1:96-110.
23. Porosity, water sorption and solubility of denture base acrylic resins polymerized conventionally or in microwave. Figuerôa RMS, Conterno B, Arrais CAG, Sugio CYC, Urban VM, Neppelenbroek KH. J Appl Oral Sci 2018; 26: e20170383.
24. The impact of fabrication techniques and materials used on the surface integrity of Ceramic Dental Crowns. Salman ZA, Hasan NH, Abdulmajeed AA. Nat J Clin Orthop 2025; 9:10-14.
25. Comparative evaluation of surface roughness and hardness of 3D printed resins. Al-Dulaijan YA, Alsulaimi L, Alotaibi R, Alboainain A, Alalawi H, Alshehri S, et al. Materials (Basel) 2022; 15:6822.